ISSN 1063-7761, Journal of Experimental and Theoretical Physics, 2012, Vol. 114, No. 6, pp. 1052–1057. © Pleiades Publishing, Inc., 2012.
Original Russian Text © E.S. Batyrshin, A.P. Krekhov, O.A. Scaldin, V.A. Delev, 2012, published in Zhurnal Eksperimental'noi i Teoreticheskoi Fiziki, 2012, Vol. 141, No. 6, pp. 1200–1205.

STATISTICAL, NONLINEAR, AND SOFT MATTER PHYSICS

On the Role of Flexoeffect in Synchronization of Electroconvective Roll Oscillations in Nematics

E. S. Batyrshin, A. P. Krekhov, O. A. Scaldin, and V. A. Delev

Institute of Molecular and Crystal Physics, Ufa Research Center, Russian Academy of Sciences, Ufa, 450075 Russia

e-mail: batyrshin@anrb.ru

Received September 29, 2011

Abstract—We describe the dynamics of zigzag oscillations in a system of convective rolls in a nematic liquid crystal above the electroconvection threshold under the action of an ac voltage with a biased position of the mean value. It is found that an increase in the contribution from the constant component leads to a substantial increase in the spatiotemporal ordering of zigzag rolls and their synchronization with the homogeneous twist mode. The results confirm the flexoelectric mechanism of locking.

DOI: 10.1134/S1063776112040061

1. INTRODUCTION

Nematic liquid crystals (NLCs) constitute one of the most attractive model systems for studying universal aspects of formation and evolution of spatiotemporal order in various nonequilibrium physical, chemical, and biological systems [1, 2]. NLCs are anisotropic liquids characterized by orientational ordering of elongated molecules. The preferred direction of orientation of NLC molecules is described by the field of director **n** [3]. Electroconvective instability occurs when a voltage exceeding a certain critical value is applied to the NLC layer enclosed between conducting substrates. In this case, a periodic system of stripes is formed representing spatially periodic modulation of the director field and of the NLC flow velocity (electroconvective rolls). Incessant activity in the study of electroconvective structures is due to the importance of analyzing the possible mechanisms of self-organization in complex anisotropic systems. The relative simplicity of measuring the control parameters (amplitude and frequency of the applied voltage) and the high optical contrast of the formed structures due to optical anisotropy of NLCs ensure considerable advantages in experimental studies of electroconvection.

The ideas put forth by Carr [4] and Helfrich [5] concerning the mechanism of electroconvection in anisotropic liquids have led to the construction of the standard electroconvection model [3, 6–9], which has been used to compute the threshold characteristics of instabilities. The instability scenario is determined by the signs of anisotropy of permittivity ϵ_a and conductivity σ_a and by the initial distribution of the director field [10, 11]. In accordance with the standard model, the necessary condition for the occurrence of electroconvective instability is the positive sign of conductivity anisotropy ($\sigma_a > 0$). The discovery of the so-called nonstandard electroconvection regime in NLCs with $\sigma_a < 0$ [11–13], for which the Carr–Helfrich convective mechanism does not operate, initiated further development of theoretical models. Nonstandard electroconvection has been explained in the model taking into account flexopolarization [14, 15] and ensuring good quantitative agreement with experimental threshold parameters. The considerable effect of flexopolarization on electroconvection was also demonstrated earlier for NLCs with $\sigma_a > 0$ [16, 17].

In contrast to the threshold for the formation of electroconvective rolls, which has been studied in detail experimentally and theoretically, the behavior of the system in the supercritical region has been studied less comprehensively. A characteristic feature of electroconvection in NLCs above the threshold for the formation of convective rolls is a large variety of secondary instabilities and scenarios of the evolution of nonequilibrium structures due to various nonlinear interactions of hydrodynamic and orientational modes. One of the most important mechanisms determining the evolution of secondary instabilities in the supercritical region is the excitation of a homogeneous (in the plane of the layer) twist mode of the director [18, 19]. It has been established that an increase in the applied ac voltage to a value above the electroconvection threshold in a planar layer of an NLC leads to excitation of the twist mode and is accompanied by the formation of so-called abnormal rolls [18, 20, 21]. In addition, the interaction of the twist mode with convective modes of rolls in an ac electric field may lead to the evolution of local oscillations between two degen-

erate states of oblique rolls (so-called zigzag rolls) [19]. The dynamics of such oscillations represents typical patterns of spatiotemporal chaos [22].

Under the action of a dc electric field, the evolution of electroconvection in the supercritical region may lead to the formation of a 2D structure in the form of a superposition of zig and zag rolls [23, 24]. The loss of stability of such a structure also leads to the development of zigzag oscillations.

A distinguishing feature of these oscillations is synchronization, which manifests itself in the generation of phase waves (viz., travelling, spiral, and target waves) [25, 26]. Some properties of zigzag oscillations in dc electric fields [27–29] have been described earlier, but the mechanism of their occurrence is still unclear.

In this study, we used the combined action of ac and dc voltages to investigate the role of the twist mode and to determine the mechanism of the spatiotemporal locking of zigzag oscillations. We study the regime of developed zigzag oscillations in electroconvection in a planar NLC layer.

2. EXPERIMENTAL

The cell had the form of a parallel-plate capacitor with transparent glass plates with a conducting SnO_2 layer deposited on their inner surfaces. Mechanical rubbing of the substrates ensured planar orientation of the director ($\mathbf{n}_0 \parallel \hat{\mathbf{x}}$), which was controlled by rotating the crystal. The cell filled with MBBA (TCI Europe) was placed into an Instec thermal chamber and on the stage of a Zeiss Axio Imager polarization optical microscope. The thickness of the NLC layer determined by the interferometric method was $d = 25 \pm 0.3$ μm. Experiments were performed at a temperature of $T = 28 \pm 0.05$°C. The intensity of light that passed through a 0.9×0.9 mm cell area was recorded by a CCD camera PCO VX44 in the xy plane of the layer with a spatial resolution of 512×512 points with a sampling frequency of 25 Hz and 256 levels of gray light. The resulting images were processed on a computer. We used an observation scheme sensitive to twist deformations of the director: the polarizer was perpendicular to the initial orientation of director $\mathbf{n}_0$, the analyzer was parallel to $\mathbf{n}_0$, and a $\lambda/4$ phase plate was installed between the NLC cell and the analyzer at an angle of 45° to $\mathbf{n}_0$ [21, 30].

A rectangular ac voltage

$$U = U_{ac}\,\mathrm{sgn}(\sin\omega t) + U_{dc}$$

with a displaced average value was applied to the cell. As the voltage source, we used an L-card-1250 digital-to-analog converter mated with a Tabor-9200 amplifier. The ac voltage frequency $\omega/2\pi = 20$ Hz corresponded to the conduction regime. For each combination of amplitudes U_{ac} and U_{dc}, sequences of images $I_0(x, y, t)$ with a length of 1024 frames were recorded. Each image in the sequence was normalized to the background image obtained at zero applied voltage:

$$I(x, y, t) = I_0(x, y, t)/I_{BG}(x, y).$$

To analyze the observed structures, we calculated the time-averaged structural factor (squared modulus of the Fourier transform):

$$\bar{S}(k_x, k_y) = \langle\left|\mathcal{F}_{\mathbf{k}} I(x, y, t)\right|^2\rangle_t.$$

The characteristics of the temporal dynamics for each sequence of images were determined from the space-averaged frequency power spectrum:

$$\bar{S}(f) = \langle\left|\mathcal{F}_f I(x, y, t)\right|^2\rangle_{x,y}.$$

3. RESULTS AND DISCUSSION

Under the action of ac voltage with an amplitude of $U_{ac} = 6$ V ($U_{dc} = 0$), electroconvective instability in the MBBA layer is observed in the form of well-known "normal" rolls (wavevector $\mathbf{k}$ is parallel to the initial orientation of director $\mathbf{n}_0$). With increasing applied ac voltage, the following sequence of transitions takes place: zigzag instability accompanied by the formation of oblique rolls ⟶ transition to "abnormal" rolls ⟶ "varicose" instability. This scenario of transitions was predicted using extended nonlinear analysis of the standard model of NLC electrohydrodynamics, which takes into account activation of the homogeneous twist mode [18, 19]. In contrast to a number of earlier studies [18, 22, 31], we observed for the first time the complete sequence of secondary instabilities.

A further increase in voltage leads to the emergence of a bimodal zigzag structure in the system, and developed zigzag oscillations are observed at $U_{ac} = 8.5$ V (Fig. 1a). Figure 1a also shows light and dark regions corresponding to the homogeneous twist mode of the director. It can be seen that in the region of a homogeneous twist mode of the same sign (light region outlined by the dashed contour), rolls of both zig and zag type exist, indicating weak correlation of the local dynamics of convective modes of the rolls and of the homogeneous twist mode.

While studying the behavior of the system under the combined action of ac and dc voltages, the values of U_{ac} and U_{dc} were varied such that the root-mean-square voltage $U_{rms} = \sqrt{U_{ac}^2 + U_{dc}^2}$ remained unchanged. For $U_{rms} = 8.5$ V, which corresponds to the regime of developed zigzag oscillations under the action of the ac voltage, an increase in dc component U_{dc} to above a certain threshold value substantially changes the oscillation pattern (Fig. 1b). The sizes of the regions occupied by rolls of the same type (zig or zag) increase considerably, which is manifested in narrowing of the corresponding peaks in the structural factor (see Fig. 1b).

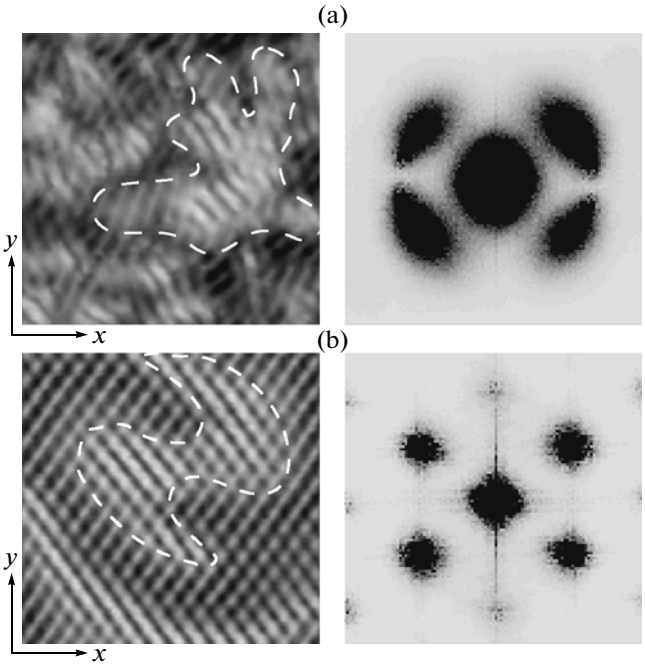

Fig. 1. Typical patterns of electroconvection (left) (0.45 × 0.45 mm region is shown) and time-averaged structural factors (right). The initial orientation of the director is along the x axis; the rms applied voltage is $U_{rms} = 8.5$ V. Large-scale light and dark regions on the images of convective structures correspond to the distribution of the homogeneous twist mode with amplitude $\pm\varphi$. The dc component U_{dc} of the applied voltage is 0 (a) and 4 V (b).

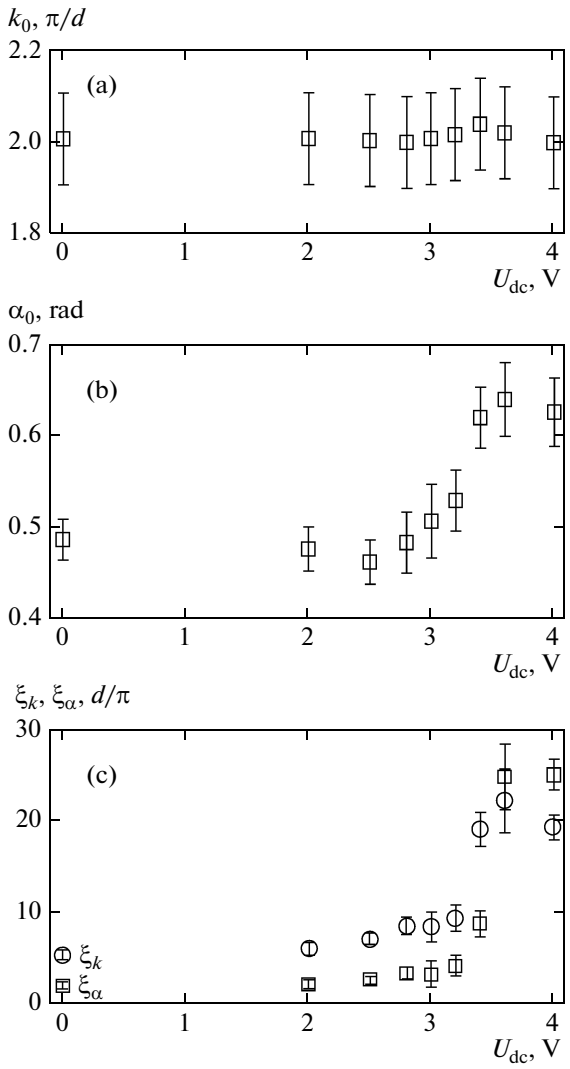

Fig. 2. Characteristics of spatial ordering of the structure for $U_{rms} = 8.5$ V and for various values of the dc component: (a) modulus k_0 of the wavevector; (b) angle α_0 of deviation of the wavevector from the x axis; (c) correlation lengths ξ_k and ξ_α.

In addition, in contrast to the behavior of the system at $U_{dc} = 0$, rolls of only one type exist in the regions with the twist mode of the same type, which indicates synchronous behavior of the convective mode of the rolls and the homogeneous twist mode. Zigzag oscillations become synchronized, and phase waves are generated analogously to the situation observed under the action of the dc voltage alone [25].

3.1. Spatial Correlations

In order to obtain a quantitative description of the spatiotemporal locking, we analyzed the profiles of the peaks in the structural factor corresponding to zig and zag rolls. The structural factor $\bar{S}(k_x, k_y)$ was approximated in the polar coordinates by the Lorentz function corresponding to the linearized amplitude Ginzburg–Landau equation for tilted rolls [8, 32]:

$$\bar{S}(k, \alpha) = \frac{S_0}{\xi_k^2(k - k_0)^2 + k_0^2\xi_\alpha^2(\alpha - \alpha_0)^2 + 1}, \qquad (1)$$

where k_0 is the modulus of the wavevector corresponding to the maximal value of $\bar{S}(k, \alpha)$, α_0 is the angle of deviation of wavevector $\mathbf{k}_0$ from the x axis ($+\alpha_0$ for zig- and $-\alpha_0$ for zag rolls), and ξ_k and ξ_α are the corresponding correlation lengths characterizing the degree of ordering of the structure (their values are reciprocal to the halfwidth of the peak at its half-amplitude). We processed peaks for zig and zag rolls and used the average value for the result. Figure 2 shows the behavior of k_0 and α_0 upon an increase in the constant component U_{dc}. Modulus k_0 of the wavevector of oblique rolls remains almost unchanged (Fig. 2a), while angle α_0 increases for $U_{dc} > 3$ V (Fig. 2b). The most significant change occurring in the system is a considerable increase in the spatial correlation lengths ξ_k and ξ_α of zigzag rolls, which begins in a threshold manner at $U_{dc} = U_{dc}^{sync} \approx 3.1$ V (Fig. 2c). This means that zigzag rolls become more ordered and correlated in the xy

plane both in period and orientation angle. The average size of the rolls of the same type is approximately $\xi_k/(\pi/k_0)$ and increases from 2–4 (at $U_{dc} = 0$) to 12–14 (at $U_{dc} = 4$ V) rolls.

3.2. Temporal Correlations

Let us now consider the temporal dynamics of zigzag oscillations. Figure 3a shows the typical time series of the local variation in intensity $I(x_0, y_0, t)$, indicating that upon an increase in dc component U_{dc}, local oscillations become more regular. To analyze the temporal dynamics of zigzag oscillations, frequency power spectrum $\bar{S}(f)$ was approximated by the Lorentz function

$$\bar{S}(f) = \frac{S_0}{\xi_f^2 (f - f_0)^2 + 1}, \quad (2)$$

where f_0 is the characteristic frequency of zigzag oscillations corresponding to the maximum of $\bar{S}(f)$ and ξ_f is the temporal correlation interval. It was found that an increase in dc component U_{dc} leads to a narrowing of the characteristic peak in the frequency power spectrum (Fig. 3b). A considerable increase in the temporal correlation interval ξ_f (Fig. 3c) almost repeats the dependences for spatial correlations. Consequently, spatial ordering in the system of oscillating zigzag rolls is accompanied by frequency synchronization. The average number of periods $\xi_f f_0$ of synchronous oscillations increases from 5 (at $U_{dc} = 0$) to 50 (at $U_{dc} = 4$ V). Frequency f_0 of zigzag oscillations also increases when $U_{dc} > 3$ V (see Fig. 3c). The increase in f_0 is apparently associated with complete locking of the zigzag modes with the homogenous twist mode, which results in a decrease in the relaxation time for rolls.

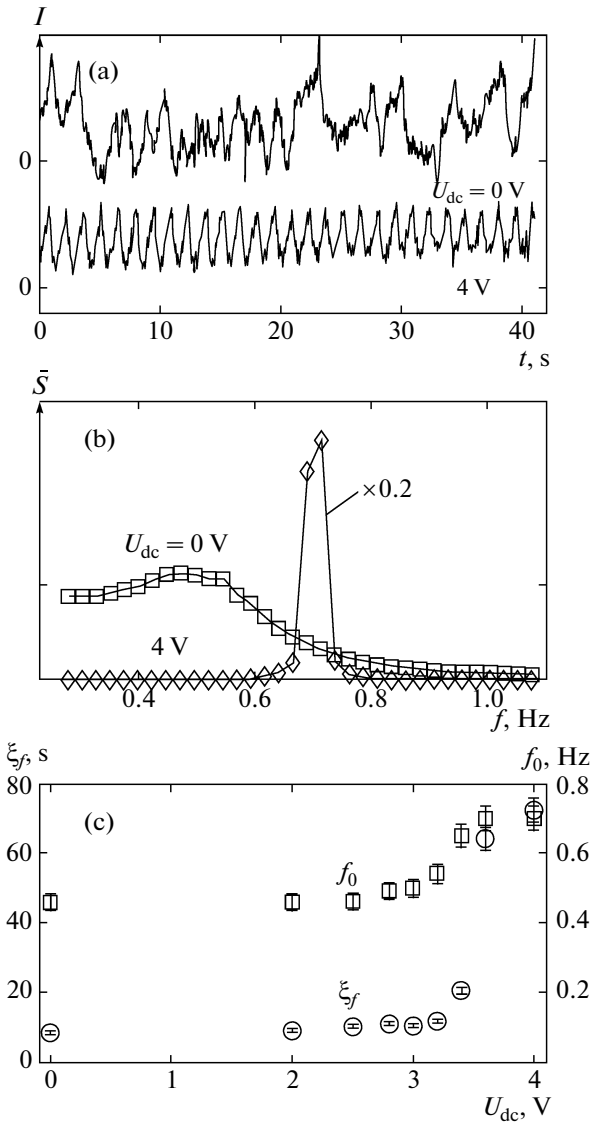

Fig. 3. Temporal dynamics of the system for $U_{rms} = 8.5$ V and for various values of dc component U_{dc}: (a) characteristic time series of the local variation of intensity; (b) space-averaged power spectra $\bar{S}(f)$ (the scales of the spectra are different); (c) dependences of the temporal correlation interval ξ_f and frequency f_0 of zigzag oscillations on dc voltage component U_{dc}.

4. CONCLUSIONS

Thus, upon an increase in the dc component of the ac voltage applied to an NLC layer, the effect of spatiotemporal ordering is observed in the system of oscillating zigzag rolls. Complete locking of spatially periodic zigzag modes with the homogeneous twist mode takes place. The fact that spatiotemporal synchronization occurs in the system only in the presence of the dc component in the applied ac voltage suggests that its mechanism is associated with flexopolarization.

From the theoretical point of view, the flexoelectric torque acting on the director and averaged over a period of the ac field is zero for $U_{dc} = 0$ because the flexoelectric response in the NLC is linear in the field [3]. The presence of the dc component $U_{dc} \neq 0$ in the voltage applied to the layer must lead to an additional static twist deformation of the director field [14, 15]. Preliminary symmetry analysis of the dynamics equations for NLCs shows that the flexoeffect developing on the background of zigzag oscillations of electroconvective rolls in turn ensures locking between the twist mode of a certain polarity and one of the types of zigzag rolls.

The flexoelectric mechanism of synchronization is also confirmed by the fact that under the action of dc voltage $U_{dc} \approx U_{dc}^{sync}$ alone ($U_{ac} = 0$), longitudinal domains oriented parallel to the initial direction of the

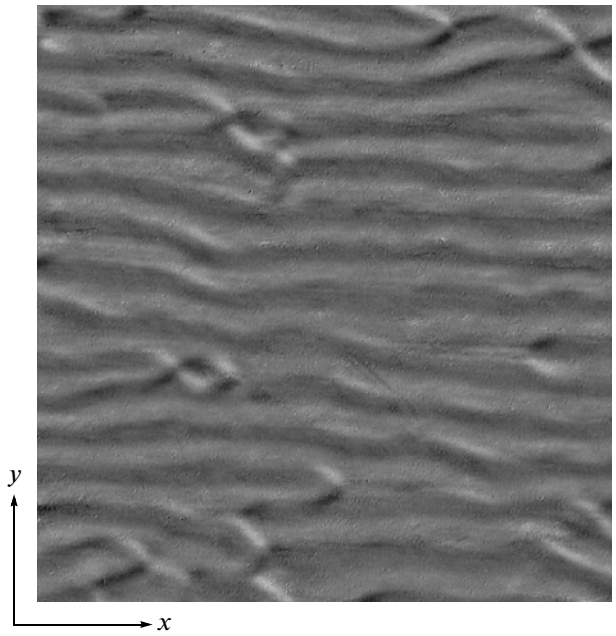

Fig. 4. Longitudinal domains in a dc electric field with $U_{dc} = 4.0$ V; the initial orientation of the director is along the x axis.

director are observed in the system under investigation (Fig. 4). It has been established that upon a change in the thickness of the NLC layer (in the interval from 15 to 70 μm), the threshold voltage for domain formation remains unchanged, while the period increases linearly with the thickness. These properties indicate that the observed longitudinal domains are flexodomains [15, 33]; their detailed investigation will be the subject of further studies.

To analyze the synchronization mechanism and the role of the flexoeffect, nonlinear analysis of the electrohydrodynamics equations for NLCs including flexopolarization is required. Another important aspect of investigations is to clarify the role of locking of convective modes with the homogeneous twist mode in the process of phase waves generation.

ACKNOWLEDGMENTS

The authors are grateful to M.V. Khazimullin and Yu.A. Lebedev for helpful discussions.

This study was financially supported by the Academy of Sciences of the Republic of Bashkortostan (project no. 3.3.3.2-2011).

REFERENCES

1. M. Cross and H. Greenside, *Pattern Formation and Dynamics in Nonequilibrium Systems* (Cambridge University Press, Cambridge, 2009).
2. *Pattern Formation in Liquid Crystals*, Ed. by Á. Buka and L. Kramer (Springer, New York, 1996).
3. P. G. de Gennes, *The Physics of Liquid Crystals* (Clarendon Oxford, 1974; Mir, Moscow, 1977).
4. E. F. Carr, Mol. Cryst. Liq. Cryst. **7**, 253 (1969).
5. W. Helfrich, J. Chem. Phys. **51**, 4092 (1969).
6. E. Dubois-Violette, P. G. de Gennes, and O. Parodi, J. Phys. (Paris) **32**, 305 (1971).
7. E. Dubois-Violette, J. Phys. (Paris) **33**, 95 (1972).
8. E. Bodenschatz, W. Zimmermann, and L. Kramer, J. Phys. (Paris) **49**, 1875 (1988).
9. S. A. Pikin, *Structural Transformations in Liquid Crystals* (Nauka, Moscow, 1981; Taylor and Francis, London, 1991).
10. Á. Buka, N. Éber, W. Pesch, and L. Kramer, in *Self-Assembly, Pattern Formation, and Growth Phenomena in Nano-Systems*, Ed. by A. A. Golovin and A. A. Nepomnyashchy (Springer, Dordrecht, 2006), p. 55.
11. Á. Buka, N. Éber, W. Pesch, and L. Kramer, Phys. Rep. **448**, 115 (2007).
12. E. Kochowska, S. Németh, G. Pelzl, and Á. Buka, Phys. Rev. E: Stat., Nonlinear, Soft Matter Phys. **70**, 011711 (2004).
13. D. Wiant, J. T. Gleeson, N. Éber, K. Fodor-Csorba, A. Jákli, and T. Tóth-Katona, Phys. Rev. E: Stat., Nonlinear, Soft Matter Phys. **72**, 041712 (2005).
14. A. Krekhov, W. Pesch, N. Éber, T. Tóth-Katona, and Á. Buka, Phys. Rev. E: Stat., Nonlinear, Soft Matter Phys. **77**, 021705 (2008).
15. A. Krekhov, W. Pesch, and Á. Buka, Phys. Rev. E: Stat., Nonlinear, Soft Matter Phys. **83**, 051706 (2011).
16. T. Tóth-Katona, N. Éber, Á. Buka, and A. Krekhov, Phys. Rev. E: Stat., Nonlinear, Soft Matter Phys. **78**, 036306 (2008).
17. M. May, W. Schöpf, I. Rehberg, A. Krekhov, and A. Buka, Phys. Rev. E: Stat., Nonlinear, Soft Matter Phys. **78**, 046215 (2008).
18. E. Plaut, W. Decker, A. G. Rossberg, L. Kramer, W. Pesch, A. Belaidi, and R. Ribotta, Phys. Rev. Lett. **79**, 2367 (1997).
19. E. Plaut and W. Pesch, Phys. Rev. E: Stat. Phys., Plasmas, Fluids, Relat. Interdiscip. Top. **59**, 1747 (1999).
20. S. Rudroff, H. Zhao, L. Kramer, and I. Rehberg, Phys. Rev. Lett. **81**, 4144 (1998).
21. S. Rudroff, V. Frette, and I. Rehberg, Phys. Rev. E: Stat. Phys., Plasmas, Fluids, Relat. Interdiscip. Top. **59**, 1814 (1999).
22. M. Dennin, Phys. Rev. E: Stat. Phys., Plasmas, Fluids, Relat. Interdiscip. Top. **62**, 6780 (2000).
23. S. Hirata and T. Tako, Jpn. J. Appl. Phys. **20**, L459 (1981).
24. A. N. Chuvyrov and V. G. Chigrinov, Sov. Phys. JETP **60** (1), 101 (1984).
25. V. A. Delev, O. A. Scaldin, and A. N. Chuvyrov, Liq. Cryst. **12**, 441 (1992).

26. V. A. Delev, O. A. Skaldin, and A. N. Chuvyrov, Sov. Phys. Crystallogr. **37** (6), 854 (1992).
27. E. S. Batyrshin, V. A. Delev, and A. N. Chuvyrov, Crystallogr. Rep. **44** (3), 506 (1999).
28. V. A. Delev, E. S. Batyrshin, O. A. Scaldin, and A. N. Chuvyrov, Mol. Cryst. Liq. Cryst. **329**, 499 (1999).
29. V. A. Delev, O. A. Scaldin, E. S. Batyrshin, and E. G. Axelrod, Tech. Phys. **56** (1), 8 (2011).
30. H. Amm, R. Stannarius, and A. G. Rossberg, Physica D (Amsterdam) **126**, 171 (1999).
31. D. Funfschilling, B. Sammuli, and M. Dennin, Phys. Rev. E: Stat., Nonlinear, Soft Matter Phys. **67**, 016207 (2003).
32. S.-Q. Zhou and G. Ahlers, Phys. Rev. E: Stat., Nonlinear, Soft Matter Phys. **74**, 046212 (2006).
33. Yu. P. Bobylev and S. A. Pikin, Sov. Phys. JETP **45** (1), 195 (1977).

Translated by N. Wadhwa